Biol. Cybern. 66, 437–441 (1992)

Biological Cybernetics

The amplitudes of unit events in *Limulus* photoreceptors are modulated from an input that resembles the overall response*

Norberto M. Grzywacz [1,2], Peter Hillman [1], and Bruce W. Knight [3]

[1] Institute of Life Sciences, The Hebrew University of Jerusalem, Jerusalem 91904, Israel
[2] Smith-Kettlewell Eye Research Institute, 2232 Webster Street, San Francisco, CA 94115, USA
[3] The Rockefeller University, New York, NY 10021, USA

Received September 7, 1991/Accepted September 18, 1991

Abstract. Light adaptation is a gain-control process that endows photoreceptors with large dynamic range. In invertebrates, this process appears to be mediated by a negative feedback that sets the amplitude of the isolated photon responses (bumps) by modulating an enzyme's rate of catalysis. This paper reports measurements of the feedback dynamics of *Limulus* from the responses to small modulations in light intensity. The responses show a noise that apparently arises from the random arrival of photons. We use a dynamic noise-analysis technique to extract the cells's frequency-response transfer function for bump amplitude. Its ratio to the transfer function for the summed response of the cell has a simple form at low frequencies. This indicates that the origin of the feedback responsible for the adaptation is at a stage temporally close to the final conductance response. Moreover, the form of the transfer function suggests feedback by a chemical agent which is removed by a single enzymatic-like stage at low light intensity and by several such stages in parallel but with a spread of time constants at high intensity.

1 Introduction

Photoreceptors continue to respond differentially to steady light at intensities that extend over six decades, although their range of response is limited to two or three decades. This large dynamic range is probably achieved by an enzymatic gain-control, which appears to be mediated in invertebrates by Ca^{2+} (Lisman and Brown 1972, 1975). In *Limulus*, the steady-state stimulus-response relation suggests that this gain-control is a nonlinear negative feedback (Grzywacz and Hillman 1988). Also, this relation suggests that the Ca^{2+} ions mediating this feedback originate at a late stage of the phototransduction chain and act cooperatively to inhibit an enzyme at an earlier stage (Grzywacz and Hillman 1988). This evidence for negative feedback, however, derives from an analysis of steady-state responses without consideration of dynamics. Previous works (Fein and DeVoe 1973) report on the time-course of adaptation following a step of light. However, their results can be interpreted in terms of the time course of adaptation only if the amplitude of the response to a superimposed test flash depends exclusively on the cell's sensitivity at the time of the test flash. This condition is unproven and unlikely. The problem may be avoided by application of a weakly-modulated stimulus as a probe. Since the sensitivity then would change only slightly, it would be monitored quite accurately by the modification of the responses. Use of a sinusoidally modulated stimulus makes possible the measurement of the frequency response *transfer function* (see accompanying paper, Grzywacz et al. 1992) which then reflects fully the dynamics of the process. Measurement of these responses, their dissection into unit events (the isolated photon responses or "bumps"), and interpretation of these results are the aims of this note. We find evidence that the adaptation is driven by a feedback which originates near the final transduction stage, and which has simple dynamics.

Since the processes of adaptation and transduction appear to be mutually dependent, an understanding of the mechanism of adaptation calls for a resolution of the conductance response into bumps. This enables us to focus on the stage on which the gain-control acts. Previous studies (e.g. Dodge et al. 1968) have shown that adaptation changes mainly the amplitude of the bump, and not its quantum efficiency or duration, over the range of intensities covered by our modulations.

In order to study the bump amplitude transfer function, we developed a technique for the analysis of non-stationary noise (Grzywacz et al. 1988) and applied

* This work was supported by grants from the Binational Science Foundation (BSF) Jerusalem, Israel and the Israel Academy of Sciences and Humanities, by NIH grant EY 1428, and by NSF grant DMS 8505442

it to the response to a sinusoidally modulated stimulus to yield the separate time dependences of the bump amplitude and rate. Because the amplitude of the stimulus modulation was sufficiently small, the system presumably behaved essentially linearly, and this enabled us to measure the formal transfer functions from the stimulus to the bump amplitude, and from the summed response to the bump amplitude.

2 Theory

The intensity of the stimulus may be represented as the real part of $I = I_0 + I_1 \exp(i\omega t)$, where $\omega/2\pi$ is the stimulus temporal frequency and $I_1 \ll I_0$. Under broad circumstances, the form of such input will be inherited by the various response variables (Brodie et al. 1978). In particular, the time dependent mean response $R(t)$ and its variance $V(t)$, obtained by averaging over several stimulus cycles, will be the real parts of $R = R_0 + R_1 \exp(i\omega t)$ and $V = V_0 + V_1 \exp(i\omega t)$. (We confirmed that, for the modulations used, the higher harmonic content of $R(t)$ and $V(t)$ was indeed inappreciable.) Also, we may assume the same response form for the bump rate and amplitude. The latter will then be

$$h = h_0 + h_1 \exp(i\omega t).$$

Campbell's Theorem (Rice 1944), which is familiar in the analysis of time-stationary shot-noise (Dodge et al. 1968), has a generalization to time-dependent shot noise (Grzywacz et al. 1988). Specialization to a time dependence that is sinusoidal with low amplitude shows that the normalized bump amplitude transfer function, $h_1(\omega)/h_0$, can be determined from data as

$$\frac{h_1(\omega)}{h_0} = \frac{V_1(\omega)\tilde{g}^2(0)}{V_0\tilde{g}^2(\omega)} - \frac{R_1(\omega)\tilde{g}(0)}{R_0\tilde{g}(\omega)} \qquad (1)$$

where the tilde indicates a Fourier transform, and where $g(t)$ is the bump time course (see Appendix). This time course may be estimated from the power spectrum (Wong et al. 1982). (The straightforward theoretical derivation of (1) convinces us that the general reservations expressed by Schnakenburg (1988) do not apply to the present analysis.)

3 Experimental methods

The preparation, stimulation, and recording under voltage clamp were as described in the accompanying article, except as follows. Under computer control, the intensity of the stimulus was sinusoidally modulated by varying the LED current. Linear responses were obtained to modulation depths of 40%; we used 25% here. The computer sampled the responses at 30.5 μs intervals and stored the averages of 128 successive samples. Cells were tested with six 30 s runs at each of five intensities, 1 log unit apart, which yielded approximately 10 to 10^5 bumps/s. Before each series at a new intensity, we allowed the cells to dark-adapt for 15 min. The modulation frequencies were 16, 8, 4, 2, 1, 1/2, 1/4, 1/8, 1/16, 1/32, 1/64, and 1/256 Hz. For frequencies above 2 Hz and intensities above 10^4 bumps/s, the variance modulation was too small to allow useful noise analysis.

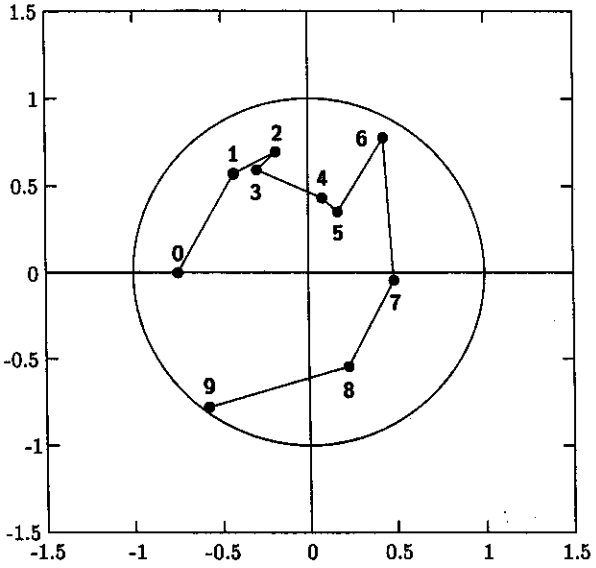

Fig. 1. The bump-amplitude transfer function of a *Limulus* ventral photoreceptor. At this background intensity, an average of about 10 bumps/s was elicited. The results are displayed in polar coordinates with the clockwise angle from the positive horizontal axis indicating phase lag and the distance from the origin representing amplitude (the dimensionless ratio h_1/h_0). The unit circle is displayed. Points 1 through 9 are, in ascending order, the results for the frequencies 1/256, 1/64, 1/32, 1/16, 1/8, 1/4, 1/2, 1, and 2 Hz. Point 0, the "zero-frequency" result, was derived from the steady-state stimulus-response curve as follows: In the intensity range illustrated in this figure, this curve has the form $R = aI^n$, with $n < 1$ (Grzywacz and Hillman 1988). If the response adaptation is ascribed entirely to the bump amplitude, the zero-frequency point may be shown to have amplitude $(1 - n)$ with phase shift π. In the cell illustrated $n \approx 0.25$. Note that this transfer function has complex features, such as the "rabbit ears" at frequencies 1/64 and 1/4 Hz. These appeared in all cells and reflect real features of the transfer function

4 Results and conclusions

Figure 1 shows, in polar coordinates, the stimulus-to-bump amplitude transfer function, $\{h_1(\omega)/h_0\}/(I_1/I_0)$, estimated from (1) after measurement under voltage clamp at one intensity. (The polar coordinate, or Nyquist, display was chosen because in it, various chemical reactions correspond to different, simple and immediately recognizable curves – see accompanying article, Grzywacz et al. 1992). This transfer function has a complicated form, as do those at the other intensities used, suggesting that there is no simple stepwise connection between stimulus and bump amplitude.

However, division of the stimulus-bump amplitude transfer function by the stimulus-response transfer function, which yields the summed response-to-bump amplitude transfer function $\{h_1(\omega)/h_0\}/\{R_1(\omega)/R_0\}$, results in a much simpler form throughout the lower frequency range. Figure 2A and B displays this function for stimuli that elicited on the average about 10 and

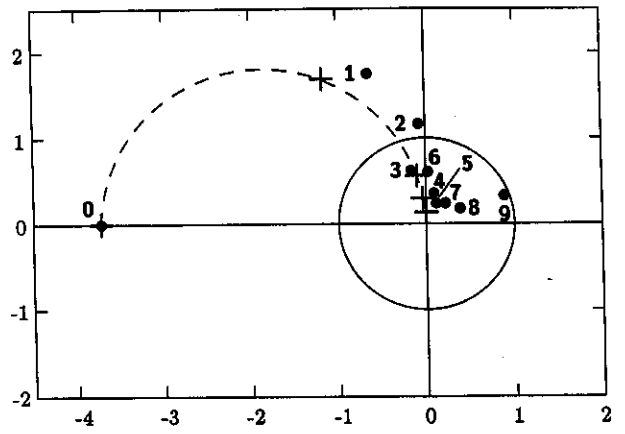

A

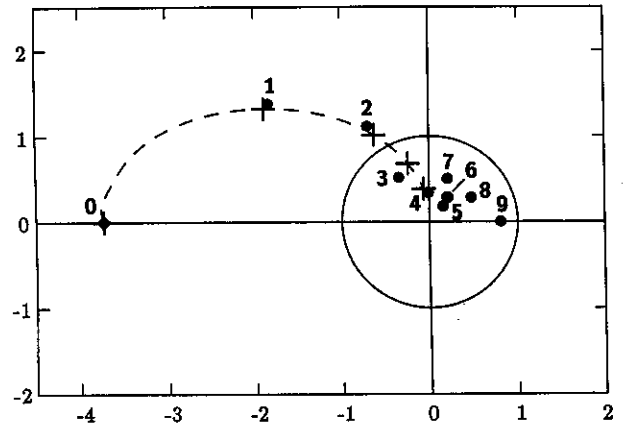

B

Fig. 2A, B. The feedback transfer function. This is the ratio of the transfer function of the bump amplitude to that of the mean response. The points are labeled as in Fig. 1. Under the assumptions of Fig. 1, the zero-frequency point can be shown to have amplitude $(1-n)/n$ and phase shift π. (A) Low background-intensity stimulus eliciting on the average about 10 bumps/s. A good fit is obtained to the low frequency data (0 to 1/16 Hz) with the dashed semicircle, which is the prediction of the model of Fig. 3A with a time constant τ of 43 s. The "+" are the predictions of the model at the frequencies of points 0 through 4. B High background-intensity stimulus eliciting on the average about 1000 bumps/s. A good fit is obtained to the low-frequency data with the dashed curve, which is the prediction of the model of Fig. 3B with time constants in the range 40–1600 s. Again the "+" are the predictions of the model at the frequencies of points 0 through 4. In both (A) and (B), the high-frequency data exhibit complex behaviour, indicating the presence of additional fast reactions controlling the bump amplitude (time constants less than 1–2 s)

1000 bumps/s respectively. Similar results were obtained at 100 and 10,000 bumps/s.

The simplicity of the low-frequency behaviour of these data suggests a casual feedback, from a stage temporally close to the final output, to the stage that controls the transduction gain. This simplicity, therefore, supports earlier conclusions that light adaptation is mediated by a negative feedback.

At the lower intensity (Fig. 2A) the low-frequency data (0 to 1/16 Hz) are well fitted by a semicircle with one end at the origin and the other on the negative part of the abscissa. Such a semicircle corresponds to a

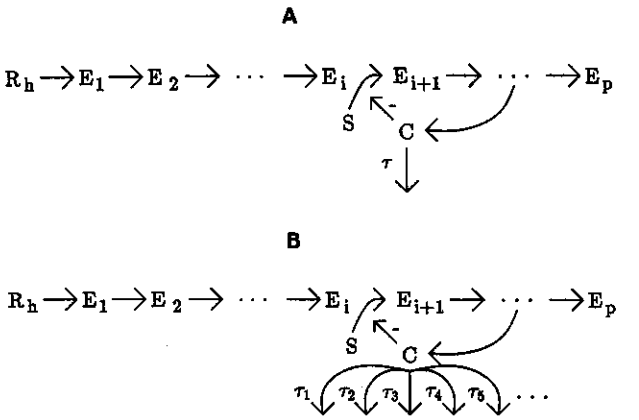

Fig. 3A, B. Models for light-adaptation. In the models described here, a chain of chemical reactions link photon absorption by rhodopsin to the ionic channels. One of the enzymatic stages of this chain is inhibited by the material C. (Evidence suggests that this material is Ca^{2+} (Lisman and Brown 1972, 1975) and that in *Limulus*, four of these ions must cooperate to induce inhibition (Gryzwacz and Hillman 1988).) The concentration of C is controlled by a stage of the chain following the inhibited enzymatic stage. Thus, C acts through a negative feedback. A The model used to calculate the dashed semicircle of Fig. 2A. In this model, the cell removes C by a single enzymatic-like stage. B The model used to calculate the dashed curve of Fig. 2B. In this model, the cell removes C by multiple parallel enzymatic-like stages. Such parallel stages may occur if, for example, the removal rate of C is spatially heterogeneous in the cell

feedback mediated by a chemical agent that is removed by a single enzymatic-like stage (Grzywacz et al. 1992), as in the scheme of Fig. 3A. A best fit, as illustrated in Fig. 2A, is obtained if the decay time constant of this agent is 43 s.

At the higher intensity, a better fit to the low-frequency data is obtained with a curve resembling a semi-ellipse with major axis along the abscissa and one end at the origin. This form is predicted from a scheme like that of Fig. 3B, in which the feedback agent is removed by several parallel enzymatic-like processes with different time constants (Gryzwacz et al. 1992). (Such behaviour occurs if, for example, the removal rate is spatially heterogeneous within the cell.) If a continuum of parallel processes with a flat distribution of time constants is assumed, a best fit is obtained with time constants covering the range of 40 to 1600 s. This fit is shown in Fig. 2B.

Results similar to these were obtained in five other cells and at two other intensities.

At all intensities, the higher-frequency data depart from these simple curves and exhibit complex behaviour. This indicates the presence of fast additional processes somewhere in the models of Fig. 3 following stage E_{i+1}, possibly in the feedback loop.

Accordingly, we offer a model for the *Limulus* ventral photoreceptor in which light adaptation is mediated by a nonlinear (cooperative) negative feedback; the feedback arises from near the response stage (although probably not at that stage); the feedback agent is removed by a single enzymatic-like process at low intensities and several enzymatic-like processes in parallel at higher intensities; and no other processes with time

constant longer than about 2 s intervene. The intensity dependence of the feedback dynamics indicates that the adaptational state of the cell affects the rates of the underyling processes.

Acknowledgements. We thank Martin Burschka for calculations and advice, and Consuelita Correa-Grzywacz for help with the figures.

Appendix: frequency response for time-dependent Campbell's Theorem

The time-dependent Campbell's Theorem derived by Grzywacz et al. (1988) yields expressions in the form of the convolution integral, which expresses a response from weighted part inputs such as:

$$R(t) = \int_{-\infty}^{\infty} S(t')g(t-t')\,dt' = \int_{-\infty}^{\infty} S(t-t')g(t')\,dt' = S * g, \tag{1}$$

where $S(t)$ is specified below. For functions S and g which vanish for negative times, the less convenient form of an integral between limits $t'=0$ and $t'=t$ is equivalent. Below we exploit the property that for constants a and b,

$$(aS_1 + bS_2) * g = a(S_1 * g) + b(S_2 * g)\,. \tag{2}$$

With Eq. (1), the time dependent Campbell's theorem states (Grzywacz et al. Eqs. (1) and (2)) that for Poisson shot arrival rate $\lambda(t)$, shot time course $g(t)$, and mean shot amplitude $h(t)$, the ensemble mean response $R(t)$ and variance $V(t)$ of the shot noise so defined will be

$$\begin{aligned} R(t) &= \int_{-\infty}^{\infty} \lambda(t-t')h(t-t')g(t')\,dt = (\lambda h) * g\,, \\ V(t) &= 2\int_{-\infty}^{\infty} \lambda(t-t')h(t-t')^2 g(t')^2\,dt' = 2(\lambda h^2) * (g^2)\,. \end{aligned} \tag{3}$$

The factor 2 in the variance appears because here we assume at all times an exponential height distribution for the stochastic variable whose mean is h, in agreement with observation (Grzywacz and Hillman 1985).

If the driving input to the system consists of a large constant part plus a small part which is time-dependent, say

$$\mathrm{I}(t) = \mathrm{I}_0 + \varepsilon \mathrm{I}_1(t) \tag{4}$$

where ε is small, then we may anticipate that variables of the system will respond similarly:

$$\begin{aligned} &\lambda(t) = \lambda_0 + \varepsilon\lambda_1(t)_1, \qquad h(t) = h_0 + \varepsilon h_1(t), \\ &R(t) = R_0 + \varepsilon R_1(t), \qquad V(t) = V_0 + \varepsilon V_1(t)\,. \end{aligned} \tag{5}$$

The products which appear in (3) may be multiplied out:

$$\begin{aligned} \lambda h &= (\lambda_0 + \varepsilon\lambda_1)(h_0 + \varepsilon h_1) = \lambda_0 h_0 + \varepsilon(\lambda_0 h_1 + h_0\lambda_1) + \ldots \\ \lambda h^2 &= (\lambda_0 + \varepsilon\lambda_1)(h_0 + \varepsilon h_1)^2 = \lambda_0 h_0^2 + \varepsilon(\lambda_0 \cdot 2h_0 h_1 + h_0^2\lambda_1) + \ldots \end{aligned} \tag{6}$$

where the terms not written are very small, that is, like ε^2 or ε^3. Thus if (5) is substituted into (3) we obtain (to order ε)

$$\begin{aligned} R_0 + \varepsilon R_1 &= (\lambda_0 h_0 + \varepsilon(\lambda_0 h_1 + h_0\lambda_1)) * g\,, \\ V_0 + \varepsilon V_1 &= 2(\lambda_0 h_0^2 + \varepsilon(2\lambda_0 h_0 h_1 + h_0^2\lambda_1)) * (g^2)\,. \end{aligned} \tag{7}$$

If ε is set to zero, (7) becomes

$$\begin{aligned} R_0 &= \lambda_0 h_0 \int_{-\infty}^{\infty} g(t')\,dt' = \lambda_0 h_0 \tilde{g}_0 \\ V_0 &= 2\lambda_0 h_0^2 \int_{-\infty}^{\infty} g(t')^2\,dt' = 2\lambda_0 h_0^2 g_0^2\,, \end{aligned} \tag{8}$$

where the brief expressions $(\tilde{g}_0, \tilde{g}_0^2)$ used to indicate the two integrals are consistent with further notation which will prove convenient below. The equations (8) state Campbell's theorem in its usual time-independent form. As the expressions (8) may be substracted from their corresponding equations in (7) the coefficients of ε in (7) likewise may be equated:

$$\begin{aligned} R_1 &= \lambda_0 \cdot (h_1 * g) + h_0 \cdot (\lambda_1 * g) \\ V_1 &= 4\lambda_0 h_0 (h_1 * g^2) + 2h_0^2(\lambda_1 * g^2)\,. \end{aligned} \tag{9}$$

Division of these expressions respectively by R_0 and V_0 now gives

$$\begin{aligned} \frac{R_1}{R_0} &= \frac{(h_1 * g)}{h_0 \tilde{g}_0} + \frac{(\lambda_1 * g)}{\lambda_0 \tilde{g}_0} \\ \frac{V_1}{V_0} &= \frac{2(h_1 * g^2)}{h_0 \tilde{g}_0^2} + \frac{(\lambda_1 * g^2)}{\lambda_0 \tilde{g}_0^2}\,. \end{aligned} \tag{10}$$

We may further specialize the input of (4) to a sinusoid with frequency $\omega/2\pi$:

$$I_1(t) = I_1(0)e^{i\omega t}\,. \tag{11}$$

In consequence the perturbations of the several response variables (Eq. 5) likewise will be sinusoidal at the same frequency. For example, the rate equation is:

$$\lambda_1(t) = \lambda_1(0)e^{i\omega t}\,, \tag{12}$$

and similarly for the other perturbation variables h_1, R_1, and V_1. In (12) a phase lag (or lead) in the crest of the output sinusoid, in comparison to the input, will be observed when $\lambda_1(0)$ is computed and is found to be a complex number. The assumption (11), and (12) which follows it, endow the response Eqs. (10) with quite specific forms for the convolutions which appear there. For example we see:

$$\begin{aligned} (\lambda_1 * g) &= \int_{-\infty}^{\infty} \lambda_1(0)e^{i\omega(t-t')}g(t')\,dt' \\ &= \lambda_1(0)e^{i\omega t}\int_{-\infty}^{\infty} e^{-i\omega t'}g(t')\,dt' = \lambda_1(t)\cdot\tilde{g}(\omega)\,. \end{aligned} \tag{13}$$

(We may recognize that the integral which has appeared and which we have briefly designated as $\tilde{g}(\omega)$, is the Fourier transform of $g(t)$. If we set $\omega = 0$ this reduces to the simple corresponding integral of (8) which we have annotated as $\tilde{g}_0$.) The equation pair (10) now finally becomes

$$\begin{aligned} \frac{R_1(\omega)}{R_0} &= \frac{h_1 \cdot \tilde{g}(\omega)}{h_0 \cdot \tilde{g}_0} + \frac{\lambda_1 \cdot \tilde{g}(\omega)}{\lambda_0 \cdot \tilde{g}_0}\,. \\ \frac{V_1(\omega)}{V_0} &= 2\frac{h_1 \cdot \tilde{g}^2(\omega)}{h_0 \cdot \tilde{g}_0^2} + \frac{\lambda_1 \cdot \tilde{g}^2(\omega)}{\lambda_0 \cdot \tilde{g}_0^2}\,. \end{aligned} \tag{14}$$

These are a pair of linear simultaneous equations which relate the pair $(R_1/R_0, V_1/V_0)$ to the pair $(h_1/h_0, \lambda_1/\lambda_0)$. They can be solved for h_1/h_0, to yield our text Eq. (1).

References

Brodie SE, Knight BW, Ratcliff F (1978) The response of the *Limulus* retina to moving stimuli: a prediction of Fourier synthesis. J Gen Physiol 72:129–166

Dodge FA, Knight BW, Toyoda JI (1968) Voltage noise in *Limulus* visual cells. Science 160:88–90

Fein A, DeVoe RD (1973) Adaptation in the ventral eye of *Limulus* is functionally independent of the photochemical cycle, membrane potential and membrane resistance. J Gen Physiol 61:273–289

Grzywacz NM, Hillman P (1988) Biophysical evidence that light adaptation in *Limuus* photoreceptors is due to a negative feedback. Biophys J 53:337–348

Grzywacz NM, Hillman P, Knight BW (1988) The quantal source of area supralinearity of flash responses in *Limulus* photoreceptors. J Gen Physiol 91:659–684

Grzywacz NM, Hillman P, Knight BW (1992) Response transfer functions of *Limulus* photoreceptors: interpretation in terms of transduction mechanisms. Biol Cybern 66:429–435 (this issue)

Lisman JE, Brown JE (1972) The effects of intracellular iontophoretic injection of calcium and sodium ions on the light response of *Limulus* ventral photoreceptors. J Gen Physiol 59:701–719

Lisman JE, Brown JE (1975) Effects of intracellular injection of calcium buffers on light adaptation in *Limulus* ventral photoreceptors. J Gen Physiol 66:489–506

Rice SO (1944) Mathematical analysis of random noise. Bell Telephone Sys J 23:282–332

Schnakenburg J (1988) Can quantum-bumps in photoreceptors be reconstructed from noise-data? Biol Cybern 59:81–90

Wong F, Knight BW, Dodge FA (1982) Adapting bump model for ventral photoreceptors of *Limulus*. J Gen Physiol 79:1089–1113

Dr. Norberto M. Grzywacz
Smith-Kettlewell Institute
2232 Webster Street
San Francisco, CA 94115
USA